

**Zeitschrift:** Eclogae Geologicae Helvetiae  
**Herausgeber:** Schweizerische Geologische Gesellschaft  
**Band:** 91 (1998)  
**Heft:** 1

**Artikel:** Jurassic ridge collapse, subduction initiation and ophiolitic obduction in the southern Greek Tethys  
**Autor:** Clift, Peter D. / Dixon, John E.  
**DOI:** <https://doi.org/10.5169/seals-168412>

### **Nutzungsbedingungen**

Die ETH-Bibliothek ist die Anbieterin der digitalisierten Zeitschriften auf E-Periodica. Sie besitzt keine Urheberrechte an den Zeitschriften und ist nicht verantwortlich für deren Inhalte. Die Rechte liegen in der Regel bei den Herausgebern beziehungsweise den externen Rechteinhabern. Das Veröffentlichen von Bildern in Print- und Online-Publikationen sowie auf Social Media-Kanälen oder Webseiten ist nur mit vorheriger Genehmigung der Rechteinhaber erlaubt. [Mehr erfahren](#)

### **Conditions d'utilisation**

L'ETH Library est le fournisseur des revues numérisées. Elle ne détient aucun droit d'auteur sur les revues et n'est pas responsable de leur contenu. En règle générale, les droits sont détenus par les éditeurs ou les détenteurs de droits externes. La reproduction d'images dans des publications imprimées ou en ligne ainsi que sur des canaux de médias sociaux ou des sites web n'est autorisée qu'avec l'accord préalable des détenteurs des droits. [En savoir plus](#)

### **Terms of use**

The ETH Library is the provider of the digitised journals. It does not own any copyrights to the journals and is not responsible for their content. The rights usually lie with the publishers or the external rights holders. Publishing images in print and online publications, as well as on social media channels or websites, is only permitted with the prior consent of the rights holders. [Find out more](#)

**Download PDF:** 29.03.2026

**ETH-Bibliothek Zürich, E-Periodica, <https://www.e-periodica.ch>**

# Jurassic ridge collapse, subduction initiation and ophiolite obduction in the southern Greek Tethys

PETER D. CLIFT<sup>1</sup> & JOHN E. DIXON<sup>2</sup>

*Key words:* Ophiolite, Tethys, Peloponesos, forearc, subduction

## ABSTRACT

The Migdhalitsa Ophiolite is the southernmost of the Hellenic ophiolites, and was emplaced on to the Pelagonian microcontinent during the Upper Jurassic from an adjacent Tethyan ocean basin. Despite its small size the ophiolite comprises a series of distinct lava sequences, erupted over a relatively short period. These principally comprise N-MORBs and basalts enriched in incompatible trace elements, generated by melting of a normal and a depleted source at a slow-spreading oceanic ridge. In contrast, small volumes of picritic and boninitic lavas suggest the ophiolite was soon placed in a forearc position above a newly initiated subduction zone. This implies overthrusting at or close to the ridge, possibly due to ridge collapse. As subduction continued the ophiolite was emplaced over the Pelagonian platform following its collision with the trench and the resultant flexural collapse of the margin. Final obduction resulted in deposition of a turbiditic and olistostromal flysch, within a flexural trough created ahead of the advancing nappe. Composition of the flysch indicates erosion of a tectonically dissected, probably imbricated, ophiolite thrust sheet in which a variety of different structural levels were exposed. Deformation during obduction was largely thin-skinned, although locally the metamorphic basement and Paleozoic carbonate cover of the Pelagonian Continent were exposed to erosion due to out-of-sequence thrusting or structural culminations. Paleomagnetic reconstructions linked with structural studies indicate obduction towards the SSW, corresponding to the ESE in Kimmeridgian times due to relative rotation of the Argolis Peninsula. It thus seems most likely that the Migdhalitsa Ophiolite was derived from the western, Pindos oceanic suture.

## ZUSAMMENFASSUNG

Der Migdhalitsa-Ophiolit ist der südlichste Hellenische Ophiolit. Er wurde vom benachbarten Tethydischen Ozeanbecken während des Oberen Jura auf den Pelagonischen Mikrokontinent aufgeschoben. Obwohl der Ophiolit komplex relativ klein ist, umfasst er eine Serie von unterschiedlichen Lavasequenzen, die in einer relativ kurzen Zeitspanne ausgebrochen sind. Diese bestehen im Prinzip aus N-MORBs und Basalten, angereichert mit inkompatiblen Spurenelementen. Sie entstanden durch das Schmelzen einer normalen und einer verarmten Quelle an einem Slow-Spreading Ridge. Im Gegensatz dazu deuten kleine Mengen an pikritischen und boninitischen Laven darauf hin, dass sich der Ophiolit bald in einer Forearc-Position über einer neuentstandenen Subduktionszone befand. Das lässt auf Überschiebungen am oder nahe am Rücken schliessen, u.U. verursacht durch einen Kollaps des Rückens. Im weiteren Verlauf der Subduktion wurde der Ophiolit auf die Pelagonische Plattform aufgelagert, nachdem diese mit dem Graben kollidiert war und daher zusammenbrach. Die endgültige Obduktion bewirkte, dass turbiditischer und olistostromaler Flysch im Trog, der sich vor der ankommenden Überschiebungsdecke gebildet hatte, abgelagert wurde. Die Zusammensetzung des Flysch deutet auf die Erosion einer tektonisch zerstückelten, wahrscheinlich verschuppten, ophiolitischen Überschiebungsdecke hin. Unterschiedliche strukturelle Niveaus waren Erosion ausgesetzt. Die Deformation während der Obduktion war weitgehend dünnchalig, obwohl das metamorphe Basement und die paläozoische Karbonatdecke des Pelagonischen Kontinents lokal Erosion ausgesetzt waren durch Aufschubung oder strukturelle Kulmination. Paläomagnetische Rekonstruktionen verbunden mit Strukturuntersuchungen deuten an, dass die Obduktion nach SSW stattfand. Während des Kimmeridge war sie nach ESE statt gerichtet wegen der Rotation der Argolis-Halbinsel. Es scheint daher am wahrscheinlichsten, dass der Ophiolit von der ozeanischen Pindos-Sutur im Westen stammt.

## Introduction

The origin of ophiolite nappes within orogenic belts has been the subject of controversy for several years. Mounting evidence from ophiolites in several orogenic belts now favors a supra-subduction zone genesis for many of these bodies (e.g. Dewey & Bird 1971; Lippard et al. 1986; Jones et al. 1991). Most recently comparisons have been drawn between “supra-

subduction” ophiolites and the origin of intra-oceanic forearcs, with special emphasis on the co-occurrence of boninite lavas (e.g. Bloomer et al., 1995). Boninites are lavas extremely depleted in incompatible elements, believed to be formed by melting of depleted mantle at shallow depths (see Crawford (1989) for a review), conditions not readily satisfied in a steady

<sup>1</sup> Department of Geology and Geophysics, Woods Hole Oceanographic Institution, Woods Hole, MA 02543, USA

<sup>2</sup> Department of Geology and Geophysics, University of Edinburgh, Edinburgh, EH9 7JW, UK

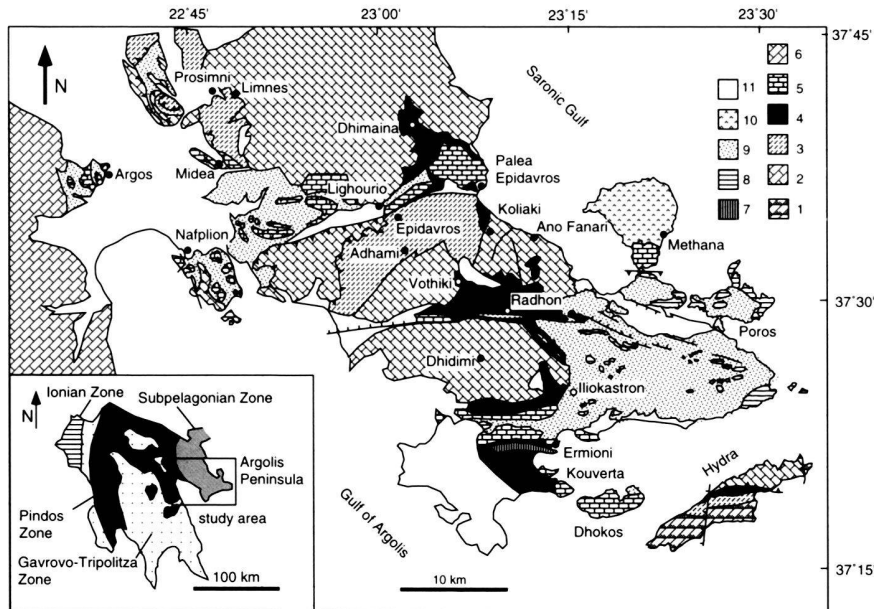


Fig. 1. Geological map of the Argolis Peninsula. Note the widespread distribution of ophiolitic rocks and their position overlying the Pantokrator Limestone platform. (1) Carboniferous limestones and sandstones; (2) Pantokrator Limestone, neritic (Mid Triassic-Liassic); (3) Adhami Limestones, pelagic (Mid Triassic-Liassic); (4) Ophiolitic units (Upper Jurassic); (5) Akros Limestone, neritic (Lower-Upper Cretaceous); (6) Pindos limestones (Upper Cretaceous); (7) Ermioni Limestones, pelagic (Upper Cretaceous); (8) Poros Formation limestones, pelagic (Lower-Upper Cretaceous); (9) Flysch (Eocene); (10) Volcanics (Quaternary); (11) Neogene-Holocene sediments. Insert shows a map of the southern Greek area showing the Isopic Zones of Greece (after Aubouin et al. 1970) and the location of the Argolis Peninsula.

state subduction environment, but which may occur in newly initiated subduction systems. Ophiolites may thus contain important information concerning the conditions existing in the oceanic crust prior to subduction initiation.

The mechanisms of subduction initiations are still strongly debated, as Casey & Dewey (1984) noted that the buoyancy of newly generated oceanic crust relative to the mantle make the initiation of subduction close to a ridge crest mechanically difficult to achieve. Nonetheless, this process was suggested for the origin of ophiolites in the eastern Mediterranean by Spray (1983) and Robertson & Dixon (1984). Alternatively, subduction initiation along transform faults was proposed as a result of work on ophiolite complexes such as the Bay of Islands, Newfoundland (Karson & Dewey 1978), and as a result of the apparent perpendicular arrangement of marine magnetic anomalies with the paleo-plate boundary in the Philippine Sea (Hussong & Uyeda 1981). In this later case however it is clear that the Palau-Kyushu Ridge, which marks the old plate boundary, cuts obliquely across the fabric in the northern Amami Plateau region, demonstrating that the early subduction zone is not simply linked to a single transform in the pre-existing Pacific lithosphere. In this paper we test models for subduction initiation in the southern Greek Mesozoic Tethys using the Migdhalitsa Ophiolite of the Argolis Peninsula, Peloponesos (Fig. 1). The Migdhalitsa Ophiolite provides a critical field area to address the initiation problem as a result of the variety of lavas erupted there over a short time span prior to obduction in the Late Jurassic.

Ophiolitic rocks are exposed throughout the Argolis Peninsula (Fig. 1). In this paper we will discuss both the widespread ophiolite-derived clastics (Potami and Dhimaina Formations;

Baumgartner 1985) and the type sections of the Migdhalitsa Ophiolite thrust sheet in central Argolis, exposed around Vothiki and Radhon (Fig. 1). Earlier work on the ophiolites of the Argolis Peninsula will be summarized and new structural and geochemical evidence will be presented to formulate a model for the evolution of this unit.

#### Previous data and interpretations

All the ophiolite units in the Argolis Peninsula lie above the drowned carbonate platform sequences of the Pantokrator/Askliopion Units (Baumgartner 1985), which represent the Pelagonian microcontinent in this area. The Pelagonian and Subpelagion Zones of eastern Greece represent a continental carbonate platform "terrane" and tectonically over-riding continental margin and ophiolite thrust sheets respectively. This terrane is positioned between two apparent oceanic suture zones, the Pindos Zone to the west and the Vardar Zone to the east (Aubouin et al. 1970). Volcanics within the carbonate platform indicate an initial rifting of the Pelagonian terrane from the northern margin of Gondwana during Middle Triassic times, similar to that inferred from rift volcanics in the Pindos Zone (Pe-Piper & Piper 1984). The precise time at which continental rifting turned to seafloor spreading is not clear because all the oceanic crust formed at this spreading center is probably now subducted. Several regional reconstructions place the onset of seafloor spreading in the Late Triassic-Early Jurassic (e.g. Ziegler 1988; Dercourt et al. 1990), and this suggestion is supported by the simple subsidence histories seen in the passive margin nappes of the Pindos Zone, implying one stage of extension progressing to full spreading (e.g. Green

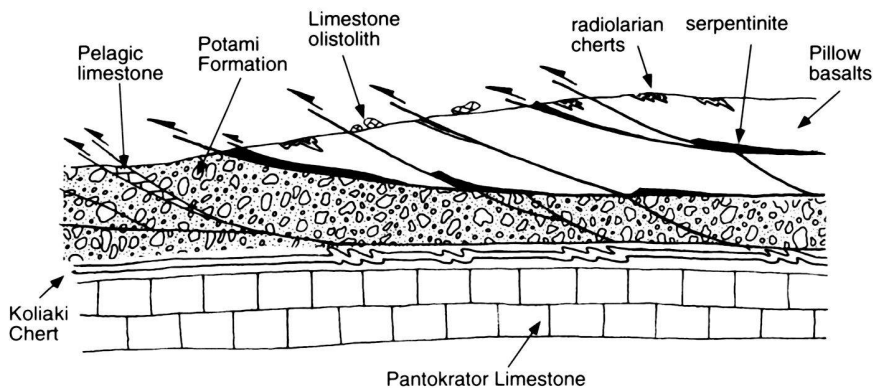


Fig. 2. Schematic cross section of the ophiolite, showing igneous imbricates structurally overlying Potami Formation deposited over the Pantokrator Limestone platform.

1983; Degnan & Robertson 1991). The history of Late Jurassic oceanic subduction and volcanism in itself requires significant oceanic spreading prior to that time.

Earlier workers (e.g. Aubouin et al. 1970, Bernoulli & Laubscher 1972) considered suturing of the Mesozoic Tethys to have taken place in the Upper Jurassic-Early Cretaceous, at the same time as ophiolite emplacement on to the carbonate platform. However, more recent data (e.g. Clift & Robertson 1989) indicate that final closure was actually a Paleogene event. Doutsos et al. (1993) suggested that while the western Pindos ocean was closed during ophiolite obduction in the Late Jurassic, the eastern Vardar ocean (referred to as the Ambelakia Ocean) remained open until the Paleogene. While there is no evidence to resolve this controversy in the Argolis area, the existence of continuous Triassic to Eocene deep water slope sequences in the Pindos Zone of northwest Peloponesos (Fleury 1980; Green 1983; Degnan & Robertson 1991), as well as Late Jurassic-Late Cretaceous deep water turbidites of the Dio Dendra Group in northwest Greece (Jones & Robertson 1991) strongly indicate that this basin remained open throughout the Mesozoic. The Pelagonian microcontinent is believed to have been accreted to the active margin of Eurasia during the Paleogene (Robertson et al. 1991).

Following the initial discovery by Aubouin et al. (1970) that the ophiolite was indeed allochthonous, Baumgartner (1985) went on to date the eruption of the lavas as Callovian (mid Jurassic) on the basis of the radiolarian fauna found in the cover sediments. Baumgartner (1985) also used trace element data from a modest sample set to infer generation of the ophiolite at a normal mid ocean ridge, a result repeated by Photiades (1986). Subsequently Dostal et al. (1991) also identified boninites within the ophiolite nappe itself, as a result of which they proposed an origin in a back-arc/inter-arc setting. It is noteworthy that the implied Late Jurassic subduction correlates well with the identification of Late Jurassic subduction-related blueschists in the Carpathians, effectively located along strike to the north of the study area (Dal Piaz et al. 1995). In the Carpathians, however, subduction is known to have culminated in collision, since the blueschists are reworked as peb-

bles in Lower Cretaceous flysch of the Pieniny Klippen Belt (Dal Piaz et al. 1995), contrasting with the open ocean in the Greek area. Moreover, while these Carpathian ophiolites represent uplifted, metamorphosed parts of the subducting plate, the Migdhalitsa Ophiolite would represent the over-riding forearc that avoided deep subduction.

Regarding stratigraphic subdivision of the ophiolitic rocks, Baumgartner (1985) split them into two parts, a lower sedimentary unit and an overlying igneous thrust sheet, the Migdhalitsa Ophiolite proper. Baumgartner (1985) further divided the sediments into two formations, a lower ophiolitic sandstone sequence, the Dhimaina Formation, and an upper olistostromal sequence, the Potami Formation, which he interpreted to represent the erosion of the ophiolite nappe during its obduction in Kimmeridgian times. He considered, in agreement with the reconstructions of Aubouin et al. (1970) and Bernoulli & Laubscher (1972), that the ophiolite had been derived from a Mesozoic Tethyan ocean basin, lying to the present east, and now represented in the Vardar Zone of northern Greece. More recently Photiades (1986) proposed an alternative three part tectonic subdivision for the ophiolite, a lower sedimentary unit, a middle dolerite and pillow basalt unit and an upper unit of ophiolitic melange. While Photiades (1986) agreed with earlier workers on the Late Jurassic origin of the ophiolite from the Vardar Zone he differed in suggesting an Eocene emplacement of the upper mélangé unit on top of the middle basaltic unit.

## Stratigraphy of the Ophiolitic Units

### *The Migdhalitsa Ophiolite*

The Migdhalitsa Ophiolite is exposed in fragments in the Palea Epidavros area, in southern Argolis (S of Ermioni), but is best preserved in central Argolis, around the villages of Radhon and Vothiki (Fig. 1). The ophiolite consists of an imbricated igneous thrust sheet overlying the clastic sediments of the Potami Formation (Fig. 2). Pillowed and massive lavas of basic to intermediate composition dominate, with pyroxene-phyric and

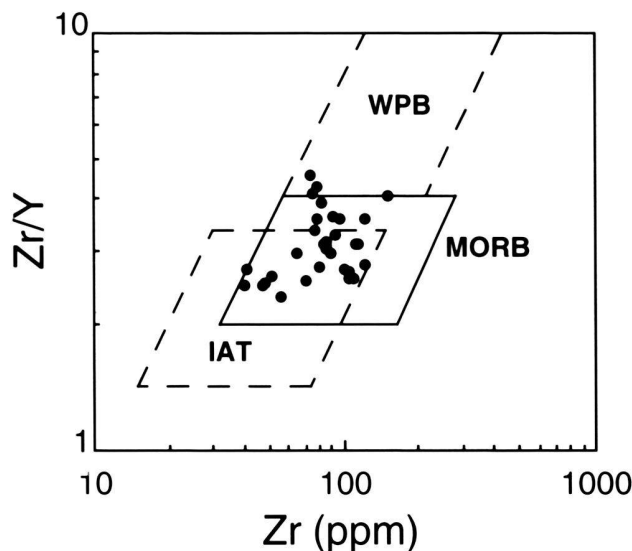


Fig. 3. Zr, Zr/Y discrimination diagram showing the Migdhalitsa lavas plotting within the MORB field but with overlaps into adjacent fields (after Pearce 1982).

feldspar-phyric tholeiites being the most abundant types (Baumgartner 1985; Photiades et al. 1989). Phenocrystic olivines are noted but are rarer and always minor components. In thin section, the basalts are commonly seen to be pervasively altered. Feldspars are frequently altered to clays, while pyroxene phenocrysts are observed altered to both hornblende amphiboles or chlorite/illite clay assemblages. The glassy matrix is also altered to a fine-grained green-brown assemblage of chlorite, epidote, phyllosilicates and green hornblende (Baumgartner 1985). Despite this, variolitic textures are observed in a number of sections, in which radiating sheaves of feldspars and pyroxenes testify to rapid quenching. In some cases the feldspars exhibit a hollow box texture, typical of quenched basaltic glasses.

Compared to an idealized ophiolite stratigraphy (e.g. Coleman 1977) several units are missing from the Migdhalitsa Ophiolite. In particular there is no development of any sheeted dike complex, or thick sequences of massive or cumulate gabbros (Baumgartner 1985; Photiades 1986). Serpentinized ultramafics and cumulate gabbros are, however, found as small tectonic intercalations at the base of the nappe, and between individual basaltic thrust sheets. Ultramafic rocks display a relict, altered harzburgitic and dunitic mineralogy, despite strong serpentinization. Relict orthopyroxene crystals and especially chrome spinels are often visible in thin section. More rarely, plagiogranites (Matthai 1989) have been reported, as well as unmetamorphosed orthopyroxenite cumulates, locally exposed as small-scale, thrust-bounded slices.

The range of lava types is markedly variable, encompassing feldspar-, olivine- and pyroxene-phyric basalts, as well as

aphyric lavas, suggesting greater variation in the extent of melting and in magma composition than is common in normal MORBs. New geochemical data (see below) indicate a wide compositional range, from picritic basalts to more evolved Hawaiites and trachyandesites, and are indicative of eruption from a magma chamber where extensive fractional crystallization had been able to take place, most typical of slow spreading centers in modern ocean basins (Nisbet & Fowler 1978). Furthermore, as deduced by Robertson et al. (1987), the presence of manganese-rich umbers overlying the lavas, rather than massive sulfides, is most similar to modern slow spreading ocean ridges (e.g. Mid-Atlantic Ridge; Scott et al. 1974) rather than East Pacific Rise-type, fast spreading ridge segments (Hekinian et al. 1983).

#### Basalt geochemistry

Previous studies of the Migdhalitsa Ophiolite indicated major and trace element geochemistries of mafic volcanics from both the Migdhalitsa Ophiolite and Potami Formation compatible with ophiolite genesis at a normal mid ocean ridge (e.g. Baumgartner 1985). More recently Dostal et al. (1991) have reported the presence of boninite lavas associated with the MORBs. We now present the results from a survey in which samples of both massive and pillowed basalts were taken throughout the type area. Only the least porphyritic or aphyric specimens were selected at each locality, in order to establish primary liquid compositions as far as possible. In each locality the visually least altered specimens were taken, often from the core of pillows, although some compositional bias may be unavoidable because of this procedure. Each sample was analyzed for ten major elements and twelve trace elements by X-ray fluorescence (XRF) at the University of Edinburgh. A selected sub-set of nine samples were also analyzed for a suite of twelve rare earth elements using an infrared coupled plasma mass spectrometer (ICP-MS) at Royal Holloway and Bedford New College, London. The results are shown in Tables 1 and 2.

#### Major element chemistry

The use of major element analyses in petrogenetic studies is severely restricted by the action of hydrothermal metamorphism and weathering on mobile elements. Using the alkali/silica classification scheme of Cox et al. (1979) the Migdhalitsa lavas are seen to range from picritic basalts to trachyandesites, with the vast majority being defined as basalts. However, the alteration evidenced by thin-section petrography means that little useful information can be determined from the major element data.

#### Trace element chemistry

A Zr against Zr/Y plot (Fig. 3) was initially used as a discriminant of original tectonic setting (Pearce 1982), which reinforced Baumgartner's (1985) original hypothesis of a MORB

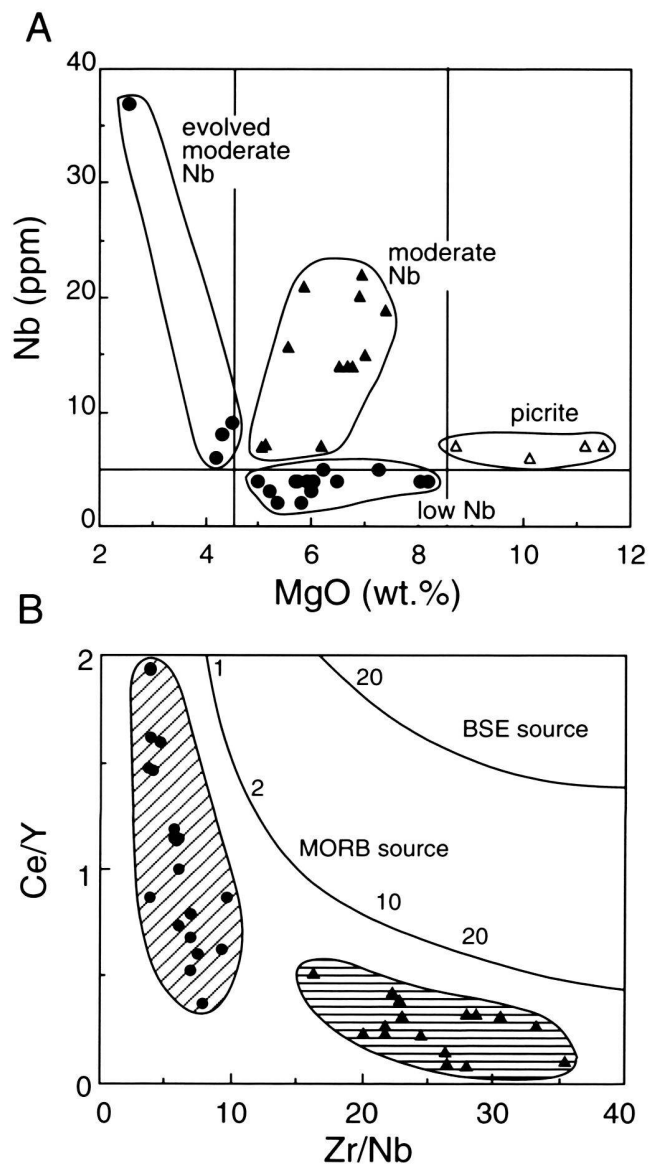


Fig. 4. (a) Nb, Mg diagram showing the division of the Migdhalitsa lavas into high Mg, low Nb, moderate Nb and evolved moderate Nb groups. (b) Ce/Y, Zr/Nb diagram showing the distribution of Migdhalitsa basalts into two major groupings, low and moderate Nb consistent with low and high degrees of partial melting.

origin, although with an inherent overlap into the subduction-related field (IAT). Further characterization of the lavas is however possible by consideration of their Mg and Nb contents. Mg concentration can be used to eliminate very evolved samples, unsuitable for further analysis, as Mg will fall rapidly as olivine is precipitated. On the other hand, the concentration of a very incompatible element such as Nb, will reflect the original degree of partial melting of the magma, but by itself will be affected by enrichment due to the fractional crystallization. Use of these two parameters may thus allow an initial

separation of rocks with different petrogenetic histories and allow elimination of evolved or cumulus enriched rocks. Figure 4a shows the presence of a broad group of basaltic lavas with MgO between 5 and 8.5%, a small picritic group with high MgO and four evolved samples with low MgO contents. Within the basaltic group a low Nb cluster is separable from a high and variable Nb cluster. As far as the outcrop pattern of these rocks is concerned it is noteworthy that there is no regular distribution of these lava groups on the ground, but they are apparently completely intermixed, magmatically or tectonically.

The evolved and picritic group were eliminated and the basaltic groups were examined further using the ratios of pairs of incompatible elements to eliminate the effects of fractional crystallization and alteration. Latin et al. (1990) have shown that Nb, Zr, Y and Ce are equally immobile in low temperature alteration processes and thus that their ratios are unaffected even if absolute values may rise due to enrichment through mobile element leaching. The same authors also demonstrate that in basalts the different degrees of incompatibility with respect to low pressure phases only begin to affect the Nb/Zr and Ce/Y ratios at fairly extreme degrees of fractionation, when MgO falls below 4%. Zr/Nb and Ce/Y can thus be used as independent measures of the extent of melting at source, which are unaffected by moderate degrees of fractionation and potentially extreme degrees of alteration. Nb and Ce are more incompatible in mantle phases than Zr and Y respectively, relative to the melt. Thus the smallest degree melts will show the largest values of Ce/Y and the smallest values of Zr/Nb. Increasing degrees of melting will cause the ratios to approach the source values, Ce/Y decreasing and Zr/Nb increasing. Figure 4b clearly shows that the initial discrimination of the basaltic rocks into two suites by their absolute content of Nb is further substantiated by the clear separation on the ratio/ratio plot into a low degree melt MORB-like group.

The moderate Nb group shows low Zr/Nb values but relatively high (up to almost 2) values of Ce/Y, indicative of very low degrees of partial melting (0.5–1.0%) of a MORB source, or 1.0–2.0% of an enriched mantle source (Latin et al. 1990). These values are far less than those predicted for N-MORB generated at a regular steady-state oceanic spreading center where the degree of partial melting inferred from trace and rare earth element data are 10–24% (McKenzie & Bickle 1988; Klein & Langmuir 1987). In contrast, the low Nb group is seen to plot with very low values of Ce/Y but with a range of Zr/Nb consistent with high degrees of partial melting (15–30+% of a MORB source, or >25% of an enriched source). The highest values of this range (55–60 Zr/Nb) are far in excess of known values for modern MORB. This is primarily due to the analytical uncertainties attached to Nb values of less than 3 ppm when determined by XRF. We do not feel able to conclude that any of these samples show the clear depletion in Nb relative to light rare earth elements (LREEs) or to mobile incompatible elements such as Ba, such as taken as indicative of a supra-subduction zone origin (Pearce 1982). It is thus concluded that lavas of the low Nb group are more likely to be prod-

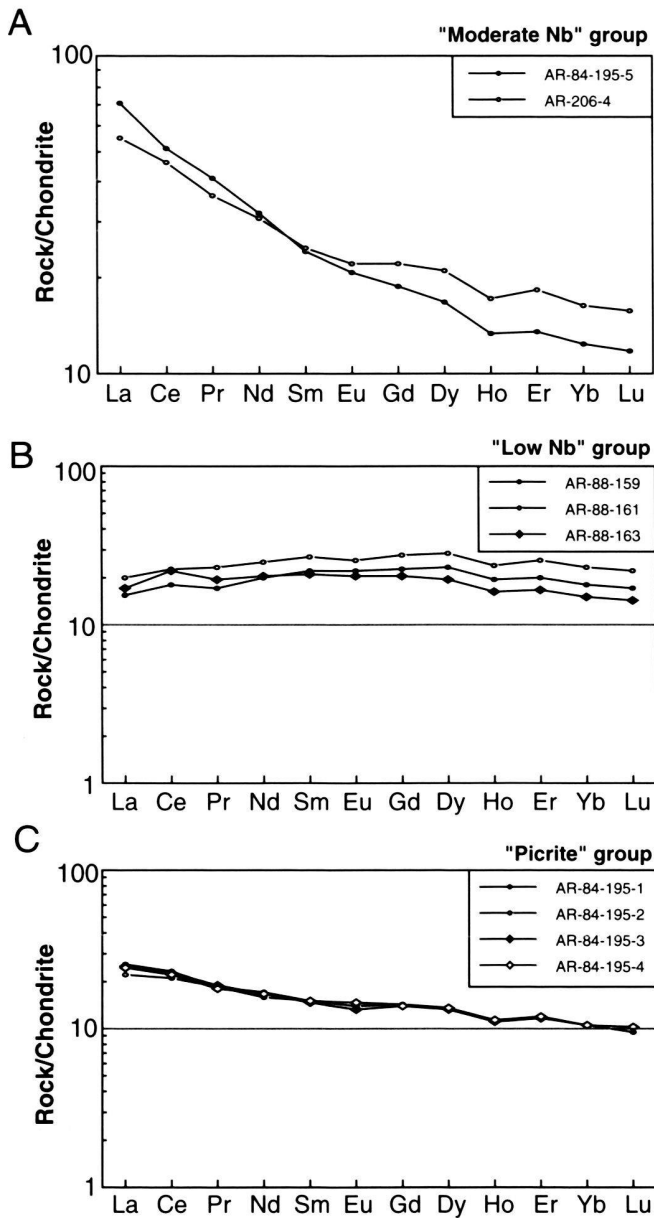


Fig. 5. Rare earth element diagram showing the three major geochemical groupings identified in the Migdhalitsa Ophiolite normalized against C1 chondrite. Normalizing values from Sun & McDonough (1989).

ucts of high degrees of partial melting at a normal mid-ocean ridge and that no conclusive evidence of above-subduction zone character is present.

#### Rare earth element chemistry

The geochemistry of the Migdhalitsa lavas can further be examined through use of rare earth elements. Figure 5 show

multi-element plots of rare earth elements normalized against C1 chondrite (values from Sun & McDonough 1989). The diagram shows three groups, the moderate Nb, low Nb and picritic basalt groups, all with their own characteristic pattern. The moderate Nb group shows a large enrichment in LREEs, both relative to chondrite and to the heavy rare earth elements (HREEs). This pattern is most commonly found in tholeiites from the modern oceans in ocean island settings. However, the low degrees of partial melt indicated by the Ce/Y-Zr/Nb diagram (<2%) would produce even higher degrees of LREE enrichment if the lavas had been derived from the enriched plume-type mantle source associated with ocean islands, as these elements are very incompatible in silicates. Typical ocean island basalts, with partial melt values of >10%, have similar LREE enrichments to the moderate Nb group, but much greater enrichment would be expected if melting was as low as 2%. Instead melting of a normal depleted upper mantle source to <2% might be expected to produce the moderate LREE enriched pattern observed. Both the other two groups show much flatter, less LREE enriched patterns. The low-Nb basalt group shows relatively flat REE plots, although enriched ten times greater than chondrite. Patterns of this form are known from low-K island arc tholeiites, as well as basalts intermediate between E- and N-type MORB, such as those found on the mid Atlantic Ridge on the edge of the Iceland hotspot (Fitton et al. 1997). However, the low Ce/Y values seen on Figure 4b would seem to preclude the involvement of an enriched mantle source. Since no subduction influence is recognized for these rocks the flat REE pattern is again explicable in terms of melting of a standard depleted upper mantle source, at slightly less than the typical 20–25% of MORBs, since this would produce a depletion of LREEs relative to HREEs. In essence the low Nb group could then be derived from the same mantle source as the moderate Nb group, but at higher degrees of partial melt. Finally Figure 5c shows the REE pattern for the picritic group. This group is characterized by very low Zr/Nb values (<0.25) and high Mg contents, corresponding to very small degrees of partial melting (1% or less of a normal depleted upper mantle). While the REE pattern does show moderate enrichment of LREEs over HREEs, this is very slight compared with expected values for derivation from either enriched or normal depleted upper mantle. In this case melting of a source which had already undergone significant depletion of its LREEs would seem most appropriate.

#### Tectonic setting and petrogenesis

Consideration of several trace and rare earth elements in the form of “spidergrams” normalized against N-MORB values (Pearce 1982) can be used to further constrain the source and melting characteristics. In this type of diagram elements are arranged along a horizontal axis on which elements mobile in aqueous fluids occupy the left-hand side (as far as Ba) and immobile the right (from Nb). Compatibility of the elements in mantle phases is arranged to increase to the right among the

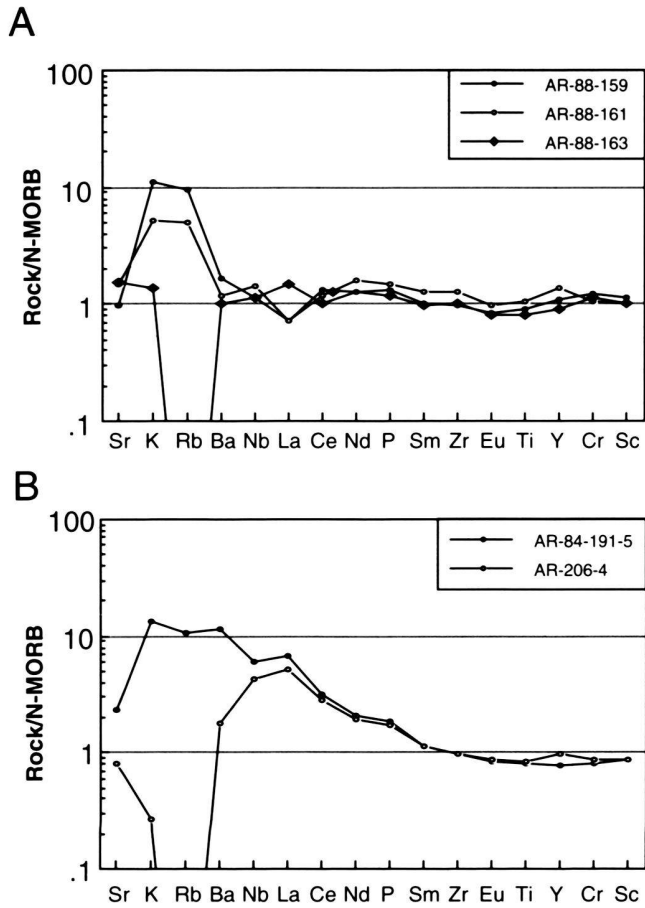


Fig. 6. Spidergrams for trace elements from: (a) moderate Nb basalts, with a within-plate type, incompatible element enriched form, (b) low Nb basalts, showing a flat MORB type trend for immobile elements. Both sets of data are normalized against N-MORB values (Pearce 1982).

immobile elements and toward the left in the mobile elements. Fig. 6a shows the low Nb group as being highly variable in the water mobile region of the spidergram, but with flat immobile trends close to the MORB line. The variability of the mobile elements can be attributed to hydrothermal alteration. Fig. 6b shows the arched pattern of typical examples from the moderate Nb group, indicating enrichment in the most incompatible elements, a characteristic of extrusives from modern oceanic within-plate settings (Pearce 1982), but also consistent with an ultra-slow spreading ridge (modern America-Antarctica and SW Indian ridges; Dick 1989). The high degrees of melting inferred for N-MORB from trace element modeling (Sun et al. 1979), or from parameterization of experimental data (McKenzie & Bickle 1989) will only apply if mantle upwelling continues virtually to seafloor. Clearly as spreading rates decline in time or space conductive cooling will progressively limit the length of the adiabatic upwelling path and so inhibit continued melting of the upper part of the mantle column. Par-

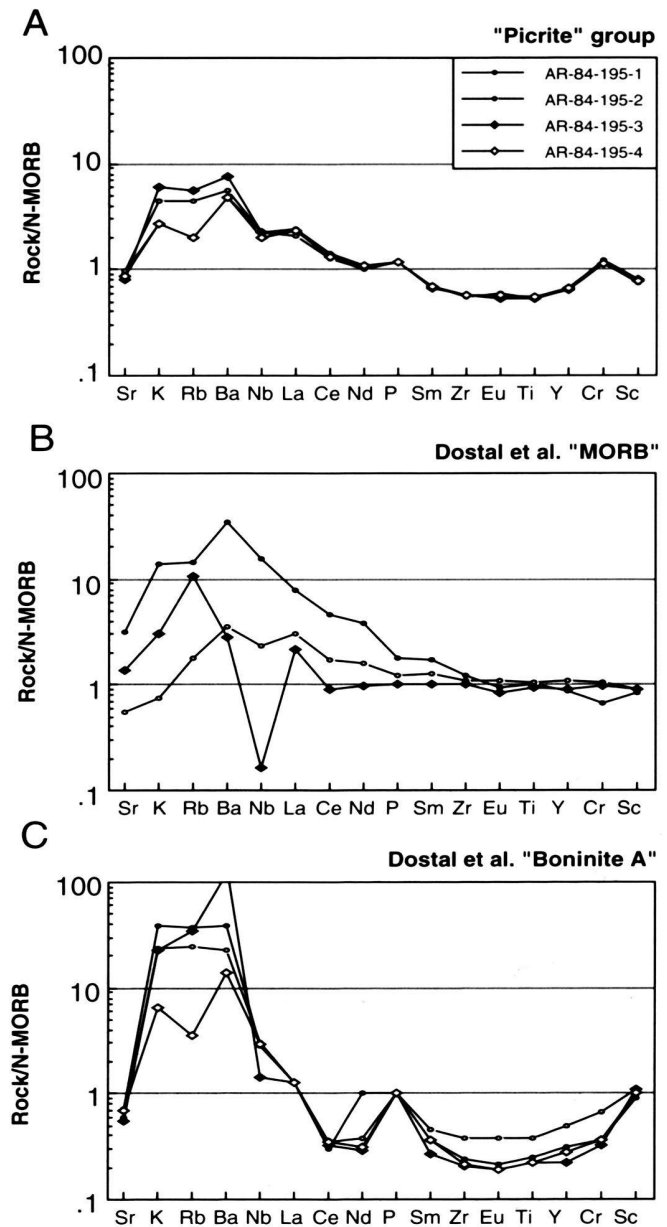


Fig. 7. Spidergrams of the high-Mg "picrite" group compared with the "Boninite A" and MORB groups of Dostal et al. (1991). Both the picrites and Boninite-A show enrichment in mobile incompatible elements but a flat depleted trend in immobile incompatible elements, giving the characteristic U-shaped trend of boninites.

tially depleted upper mantle will continue to rise but will be too cool to melt. In reality spreading at very low rates may be via intermittent rifting episodes in which this still fertile mantle is rapidly decompressed and yields small melt fractions before cooling back onto a conductive geotherm at a higher level. A process such as this may explain the distinctive shape of the trace-element patterns in Figure 6b which show some depletion in the least incompatible trace-elements Ti and Y, imply-

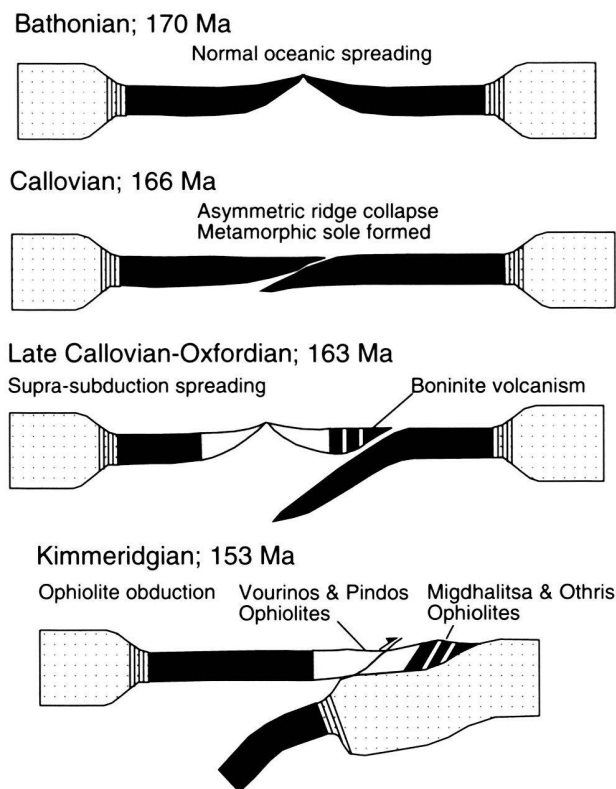


Fig. 8. Schematic genesis and obduction of the Hellenic ophiolites, showing origin of the Migdhalitsa Ophiolite at the original spreading ridge followed by ridge collapse and supra-subduction zone spreading of the Pindos and Vourinos ophiolites.

ing that a small degree of melting of an already partially depleted source has occurred. In contrast basalt from plume sources or early rift episodes, will generally show enrichment in all incompatible elements relative to N-MORB, as the source in these cases will generally not be more depleted than a regular asthenospheric MORB source.

It is noteworthy that the basalt groupings identified above are not the same as Dostal et al.'s (1991) grouping into one MORB and two sets of boninites. Plotting of Dostal et al.'s data as spidergrams (Fig. 7b and c) shows that his MORB group includes both flat and arched trends similar to our low and moderate Nb groups. The boninite groups, with their typical U-shaped trend in the immobile elements bare some similarity to our high-Mg "picritic" group (Fig 7a). The picritic group in particular is most similar to Dostal et al.'s "A" group of boninites, as these show the least depletion of Sm, Zr, Eu, Ti and Y compared to MORB. The fact that the Cr content of the picritic basalts is effectively the same as MORB points to these depletions being the result of melting of a previously depleted source, rather than the result of fractional crystallization, as suggested by the REE plots. None of the lavas ana-

lyzed as part of this study show the very high degrees of depletion shown by Dostal et al.'s "B"-group of Boninites, which are considered to form a separate group not sampled by this study.

The presence of an incompatible-enriched signature to the moderate Nb group basalts is of particular importance to any tectonic reconstruction. Although normally associated with intra-plate volcanism these lavas seem unlikely to represent a volcanic seamount carried on the back of the ophiolite, since apart from the geochemical evidence cited above, it is noteworthy that these lavas do not differ at outcrop in appearance or sedimentary cover from the MORB-type lavas. With the current data it must be assumed that most of the volcanic activity took place over a short period of time during the Bathonian-Callovian. The geochemical data cited above point to both the low- and moderate-Nb basalt groups both being generated as a result of low and very low degrees of partial melting of a standard LREE depleted upper mantle source, probably at a slow spreading mid ocean ridge.

#### *Boninites and asymmetric ridge collapse*

Further clues to the tectonic setting of the ophiolite genesis come from the presence of boninite lavas within the Migdhalitsa Ophiolite (Photiades 1989), as well as within the ophiolite sheet of Aegina island (Dietrich et al. 1987), located 20 km north of the Argolis Peninsula. In the modern oceans boninites have been identified in supra-subduction zone settings, usually in forearc regions of some newly initiated island-arc systems (e.g. Mariana forearc; Cameron et al. 1979). While models for ophiolite obduction differ in their rooting of the Subpelagonian ophiolites in the Pindos or Vardar Zones, the stratigraphy of the Pelagonian Zone suggests only one obduction event at the end of Jurassic times in the southern Greek area (Aubouin et al. 1970; Celet & Ferrière 1978). The Aegina and Argolis ophiolites may thus be considered to form parts of a single ophiolite thrust sheet. Some of the less depleted boninites, such as the low degree partial melt, „picritic“, group of this study, may have formed as a result of remelting of mantle from which a small melt fraction had already been extracted (e.g. the source of the moderate-Nb basalt group). Such a process might be envisaged during a pulse of extension at a slow-spreading, dying ridge axis. However, the presence of highly depleted, high partial melt fraction boninites in Aegina and the Migdhalitsa Ophiolite (e.g. Dostal et al.'s "B" group boninites) suggest that the ophiolite was located in or near a forearc region, at or shortly after its genesis at the mid ocean ridge. Moreover, the conditions necessary for formation of boninites (Crawford 1989) indicate that this magmatism probably occurred shortly after the initiation of subduction close to the ridge. If the boninites are the same age as the low- and moderate-Nb basalts this would indicate that the Migdhalitsa spreading center was located in a supra-subduction zone setting. Alternatively, if the boninites post-date the main sequence of MORB-type volcanism then the most suitable model would in-

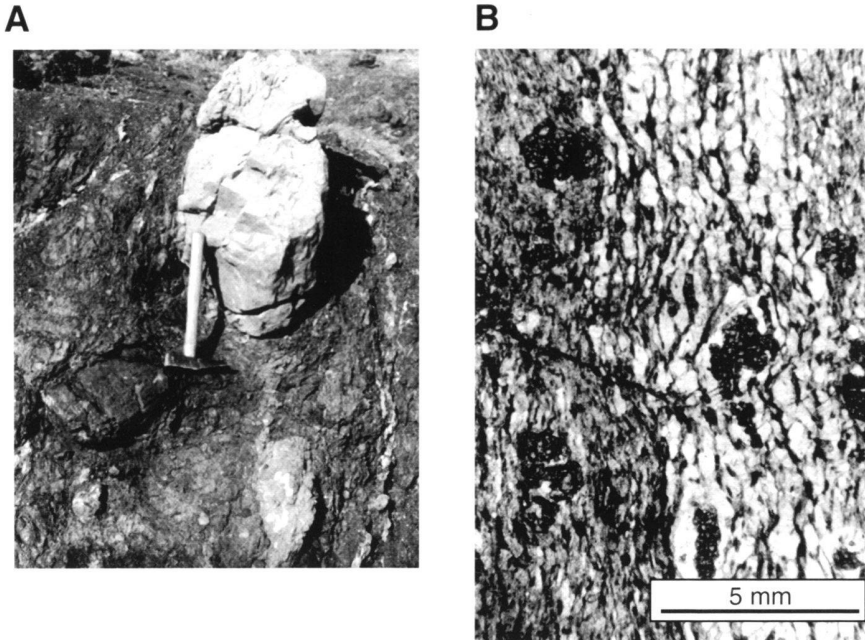


Fig. 9. (A) Photograph of Potami Formation olistostrome at Kouverta Beach, S of Ermioni. Note the blocks of radiolarian chert and quartzose sandstone enclosed in scaly cleaved shale. (B) Photomicrograph of garnet/mica/quartz schist from metamorphic thrust sheet, Palea Epidavros.

volve the initiation of subduction within N-MORB crust and the eruption of boninites in a fore-arc position of the new subduction zone (Fig. 8), similar to the Eocene of the Bonin/Mariana arc (Natland & Tarney 1979). Overthrusting close to the ridge would isolate the youngest lavas created at the ridge in a fore-arc region, comparable to the MORB-type forearc suggested for the Semail (Lippard et al. 1986) and Pindos Ophiolite nappes (Jones & Robertson 1991). Since boninites are typically found in forearc settings where N-MORB volcanism is unknown it is highly unlikely that boninite volcanism predated N-MORB volcanism.

It is possible that if subduction was actually initiated at the ridge crest, then the ridge activity would die back progressively to give smaller melt fraction lavas of the type seen (moderate Nb basalts) prior to subduction. Ridge overlap would then lead to subduction and a renewed pulse of wet remelting of depleted lithosphere, which, given slab roll-back, would generate the other Hellenic ophiolites along a supra-subduction zone spreading center in a "backarc" position to the MORB and enriched-MORB forearc remnant of the Migdhalitsa Ophiolite (c.f. Robertson & Dixon 1984; Fig. 8). The position of the MORB and enriched-MORB lavas in the forearc might also explain their present association with boninites, as these would be expected to be erupted in the situation of hot oceanic lithosphere being subducted below hot oceanic lithosphere, which would occur following ridge collapse. While no supra-subduction zone crust is known from the Migdhalitsa Ophiolite, the Vourinos and Pindos Ophiolites of northern Greece appear to represent this portion of the ophiolite. As the nature of boninite petrogenesis is still not understood in detail it is possible

that subduction initiation in the Migdhalitsa Ophiolite occurred along a transform boundary and that N-MORB volcanism significantly predated boninite extrusion. We consider this less likely because of the chemical evidence suggesting the generation of low melt fractions during the slowing of oceanic spreading. This situation is less likely to have occurred during the formation of a random piece of oceanic crust along a transform plate boundary or fracture zone, whose crust was probably generated during steady-state spreading prior to subduction initiation. Nonetheless, high resolution radiometric dating (e.g.  $^{40}\text{Ar}/^{39}\text{Ar}$ ) would be necessary to conclusively reject this possibility.

In summary, the geochemistry supports an origin for the Migdhalitsa Ophiolite at a slow spreading ocean ridge. The presence of highly depleted boninites further suggests that the ophiolite was placed in a forearc position shortly after spreading. This is different from other Hellenic ophiolites, such as Vourinos and Pindos which contain basalts of island arc tholeiite character (Jones & Robertson 1991; Noiret et al. 1981; Becaluva et al. 1984) and are inferred to have been generated in a supra-subduction zone setting. Only the Othris Ophiolite (Hynes 1974) is also known to have abundant MORB-type basalts. Collectively the chemical data place the Hellenic Ophiolites, including Migdhalitsa, in the over-riding plate of the Jurassic subduction zone. This in turn constrains the tectonics of obduction, effectively ruling out any possibility that the Migdhalitsa sheet can be considered as some sort of accreted flake of the subducting plate, and favouring simple obduction due to trench-passive margin collision, as documented in Oman (Lippard et al. 1986).

## Potami and Dhimaina Formations

Lying at the base of the ophiolite sequence and tectonically overlain by the basaltic thrust sheet (Fig. 2), the Potami and Dhimaina Formations, as defined by Baumgartner (1985), comprise up to 600 m of sheared sandstones and debris flow conglomerates respectively. Compared to the Migdhalitsa Ophiolite, discussed below, there is a greater diversity of lithologies identified within the clastics, including several common ophiolitic rock types (e.g. gabbros) which are rare in the thrust sheet itself and some rocks (e.g. metamorphic sole rocks, pyroxenites) which are absent from the thrust sheet altogether.

The debris flows typically comprise poorly sorted, matrix-supported conglomerates of red chert, basalt, serpentinite, limestones, gabbro and orthopyroxenite blocks within a friable, red, shaley matrix (Fig. 9a; Baumgartner 1985; Photiades 1986; Matthai 1989). Of particular interest is the presence of basalts within the Potami Formation, whose trace element geochemistry indicates a subduction zone influence in their petrogenesis. As well as island arc tholeiites, Photiades (1989) reported the presence of boninite lavas.

Mapping of the Potami Formation in southeastern Argolis (5 km S of Ermioni, at Kouverta Beach; Fig. 1) has identified a thick succession ( $\approx 30$  m) of relatively undeformed, massive, coarse-grained quartzose sandstones, with rare interbeds of shale. This is both over- and underlain by ophiolite-derived debris flows, but contains very little ophiolitic material itself. Interbedding of the quartzose sandstones with debris flows constrains the age of deposition of these sands to being within the range of deposition of the Potami Formation (i.e. Kimmeridgian; U. Jurassic). In thin section, the quartz grains appear sub-angular in outline and almost all show development of sub-grains or undulose extinction, indicative of recrystallization under high stress and suggestive of derivation from a metamorphic terrain, rather than recrystallization *in situ*. This is consistent with the fact that the enclosing muddy matrix only shows a weak scaly cleavage, incompatible with post-depositional metamorphism. Carbonate sediments derived from the erosion of the platform are much more abundant in this area than in other parts of the Potami Formation. Clasts of oolitic and bioclastic limestone, as well as pink micritic limestones are commonly observed. In particular, newly discovered bioclastic grainstones found in a block (3 m across) within ophiolitic debris flow conglomerates have yielded a microfossil assemblage dating sedimentation within the Djouflian or Dorashamian stages of the Permian (Vachard et al. 1993). The only known sources for this material are the Permo-Carboniferous shelf limestones cropping out on Hydra island (Fig. 1; Romermann 1968).

### *Interpretation of the Potami Formation*

The Potami Formation is interpreted to be largely the product of deposition by debris flows due to the matrix-supported na-

ture of the sediment and the lack of internal grading or bedding. The presence of many ophiolitic lithologies in the Potami Formation is considered to represent erosion of a dissected ophiolitic nappe during its obduction. The presence of chrome spinel clasts within Dhimaina Formation sandstones (Baumgartner 1985), as well as the diversity of clasts found as blocks within the Potami Formation, suggests that rocks from below the Moho were already exposed within the ophiolite early during the process of obduction. The Argolis sequences compare with *mélange* units beneath the Bay of Islands Ophiolite of Newfoundland (e.g. Milan Arm *Mélange*; Williams 1975), which contain serpentinite, basalts, amphibolites, gabbro, diorite and pyroxenite, believed to have been deposited in a fore-deep ahead of an advancing nappe.

The presence within the Potami Formation of lithologies normally found only in the lower oceanic crust (e.g. gabbro cumulates) or below the petrological Moho (altered harzburgites, chrome spinels and dunites) requires a mechanism to expose deep levels to erosion at an early stage of the obduction. Although diapirism of the serpentinitized ophiolite mantle could expose ultramafics during emplacement (e.g. Cyprus; Gass & Masson-Smith 1963) tectonic dismembering of the ophiolite, due to normal faulting at the oceanic spreading center and thrust faulting during obduction are also likely to have been important. While extensional unroofing of deep levels of the ocean crust is well documented at ocean ridges (Dick 1989), evidence for imbrication of ophiolite sheets within the ocean basin, prior to final obduction, is also known from other Tethyan ophiolites, such as the Pindos Ophiolite of northern Greece (Kostopoulos 1989; Jones & Robertson 1991). Here a peridotite thrust sheet tectonically overlies crustal sequences, due to out-of-sequence thrusting during obduction. Mass wasting, gravity slumping and erosion of an imbricated thrust stack would then allow deep-seated rocks to be exposed at the surface and so eroded into the Potami Formation. A scenario involving imbrication within the ocean basin is further suggested by the stratigraphy of the Migdhalitsa Ophiolite exposed today. In particular, the presence of pillow basalts, originally formed near the top of the ophiolite and now thrust directly over olistostromes (Fig. 2) would require the tectonic excision of the underlying crust and mantle rocks by out-of-sequence thrusting, unless the Migdhalitsa Ophiolite represents a part of the ocean crust where the original detachment thrust cut up-section into the extrusive sequences on its way to the surface (c.f. Aspropotamos Complex, N. Greece; Jones et al. 1991).

In contrast to the rest of the Potami Formation, the quartzose sandstone interbeds within the Potami Formation, south of Ermioni and blocks of greywackes at Palea Epidavros (Photiades 1986) must be derived from a continental source. The basement of the Pelagonian Zone is the most likely source, as it forms the only potential block capable of being uplifted and consequently supplying material on to the Argolis platform at this time. Other metamorphic blocks in the Aegean area were separated from the Pelagonian Zone by open Tethyan seaways at this time. The presence of these sandstones within the Pota-

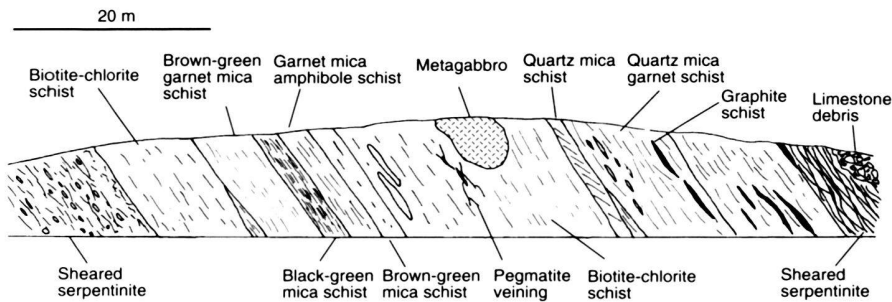


Fig. 10. Cross section of the metamorphic thrust sheet on the Lighourion/ Palea Epidavros road. Note the large competent block of gabbro in the center of the cutting.

mi Formation indicates that the basement was exposed during the process of obduction, possibly due to thrusting or erosion of a structural culmination, not exposed within the Argolis Peninsula.

### Tectonic mélangé; Metamorphic rocks

Directly beneath the ophiolite, and in contrast to the sedimentary olistostromes of the Potami Formation, a number of small-scale thrust sheets of basalt and serpentinite are found interthrust in a tectonic mélangé unit. It is important to note that this mélangé, lying below the igneous thrust sheet, is not the same as the Eocene mélangé proposed by Photiades (1986), which he considers to overlie the ophiolite. Of special interest is a slice of quartz-garnet-mica schist and interthrust metabasites and gabbro, exposed in a 60 m long road cutting close to Palea Epidavros (Photiades 1986; Figs. 1 and 10). This slice is bounded on top and bottom surfaces by sheared serpentinite, demonstrating its tectonic origin. Compared to the low-grade metamorphism of the Potami Formation, the metamorphic sheet dominantly comprises strongly foliated mica schists (muscovite, chlorite and biotite, altering to chlorite). The metasedimentary units show strained, polycrystalline quartz, with clear intergranular sutured contacts and common crenulation of mica layers (Fig. 9b). Additionally, there is a strong brittle fracture-cleavage cutting the crenulation cleavage. In some samples fine grained micaceous layers appear to represent areas of altered aluminosilicate in association with tourmaline and epidote. Metabasic intercalations exposed at Epidavros (Fig. 10) show an assemblage of zoisite, clinozoisite, plagioclase and biotite, partially altered to chlorite. Metamorphism in the epidote/amphibolite facies is inferred from the presence of almandine garnets and epidote/zoisite assemblages within these rocks (Fig. 9b). This clearly demonstrates an earlier metamorphic history of the sheet before its late stage incorporation by thrusting into a tectonic mélangé beneath the ophiolite. Significantly much of its composition appears to be most compatible with a pelitic or psammitic protolith, although now interleaved with gabbro.

### Geochemistry of the metabasites

Two specimens taken from metabasic rocks of the Palea Epidavros metamorphic sheet were analyzed for ten major elements and twelve trace elements by X-ray fluorescence at the University of Edinburgh.

The major element chemistry of these specimens shows that they are of basic composition ( $\text{SiO}_2 = 54.3\%$  and  $49.7\%$ ), although Mg is relatively low (3.67% and 3.45%) suggesting an evolved character. Investigation of the petrogenesis is however possible through use of multiple trace elements in a „spidergram“. Figure 11 shows a 14 element MORB-normalized spidergram (Pearce 1982) in which both specimens have a strong arched profile, due to enrichment in the most incompatible elements. This is a characteristic of basalts erupted in modern within plate settings, derived either by melting of an enriched mantle source (plume) or from small degrees of partial melting of a normal depleted upper mantle source, or both. For comparison typical plots for tholeiitic Hawaiian basalts from Kilauea and more alkalic basalts from Hualalai are

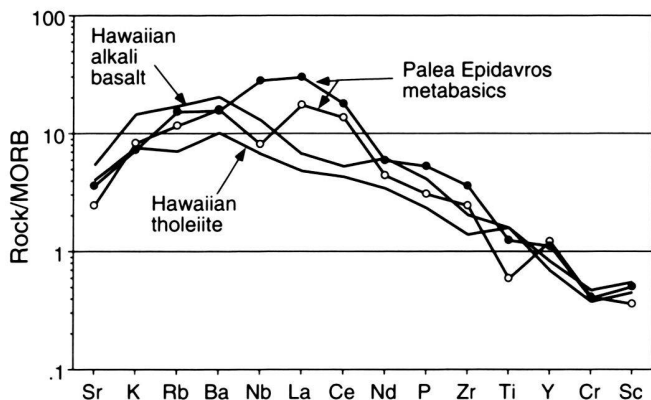


Fig. 11. Trace element spider diagram for Epidavros metabasic rocks, showing the arched within-plate signature of both specimens and their similarity to modern alkali basalts of the Azores (Pearce 1982).

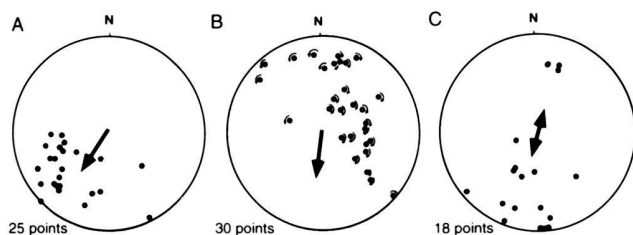


Fig. 12. Stereographic projection of (a) Poles to shear fabrics within basalts of the Migdhalitsa type area. Note clear southwest sense of shear; (b) fold hinges, with sense of asymmetry indicated, within ribbon radiolarites both from the sedimentary cover and the underlying platform sequences; (c) slickensides on emplacement-related thrusts within the Migdhalitsa type area. Large arrows show the inferred direction of tectonic transport.

shown (data from Basaltic Volcanism Study Project 1981). The latter type appears to be the closest to the Epidavros specimens. Significantly the mobile trace elements on the left hand side of the diagram form a smooth continuation of the curve and do not seem have been greatly altered by hydrothermal or metamorphic demobilization. Mafic igneous rocks with similar, within-plate chemistries are found as thrust slices under the Oman Ophiolite (Haybi Volcanics; Lippard et al. 1986) and as blocks in the sub-ophiolite mélangé of the Pindos Ophiolite (Jones & Robertson 1991).

The origin of this slice of metabasic and metapelitic amphibolite within the Potami Formation is important to understanding the obduction process. Photiades (1986) suggested that the schists are derived from the crystalline basement of the Pelagonian Zone, exposed to the northeast and presumed to underlie the Argolis Peninsula itself. This however seems unlikely, as the occurrence of metabasics and gabbro, in association with the metasediments, is incompatible with the known lithologies from the Pelagonian Zone (Celet & Ferrière 1978). Instead we interpret the metabasites and gabbro of the sheet to be remnants of an original metamorphic sole to the ophiolite generated at depth shortly after the start of intra-oceanic thrusting (i.e. Oxfordian-Kimmeridgian). The inferred epidote/amphibolite metamorphic facies is also found in the high temperature soles to the Pindos, Oman and Bay-of-Islands Ophiolites (e.g. Williams 1975; Woodcock & Robertson 1977; Malpas 1979; Searle & Malpas 1982). The metasedimentary (quartz-mica) portions of the sheet would then represent ocean floor sediments, which were over-ridden and metamorphosed by the hot ophiolite sheet as obduction proceeded. The quartzose composition of these rocks implies an original derivation by erosion of adjacent continental areas. During obduction this composite sheet would have been at the base of the ophiolite nappe and thus vulnerable to tectonic erosion and incorporation into tectonic mélangé.

## Structural evolution

Regarding the large scale structure of the ophiolite, we consider the two part scheme of a lower sedimentary unit and an over-riding igneous thrust sheet as proposed by Baumgartner (1985) to be the most appropriate. Under the scheme of Photiades (1986) an upper mélangé unit was emplaced on top of the middle igneous unit during the Upper Eocene, probably related to rethrusting during final collision in the Greek Tethys (Clift 1992). However, in all cases where ophiolitic material is found tectonically overlying Tertiary flysch, including Photiades' type section on the Lighourion-Palea Epidavros road, this ophiolitic material can be attributed to either of the two lower units. The upper tectonic unit of Photiades (1986) is always seen unconformably overlain by Cretaceous carbonates. This unit thus does not represent an important structural subdivision of the ophiolite but is merely the result of Tertiary thrusts exploiting the structural weakness along the unconformity between Cretaceous carbonates and the ophiolitic debris. Locally the thrusts have cut below the unconformity and incorporated pieces of olistostrome or basalt into the thrust sheet. As such the upper unit can be considered to be locally rethrust slices of the Migdhalitsa Ophiolite, Potami Formation or Dhimaina Formation.

Vrielynck (1982) and many previous workers considered the ophiolite to be derived from the eastern Vardar Zone, although without any convincing structural evidence from the Argolis Peninsula itself. Baumgartner (1985) presented evidence of fining and thinning of the Potami Formation towards the west as proof of an emplacement from the east, although erosion of the Potami Formation following obduction means that this evidence can be considered patchy at best. More recently Photiades (1986) and Matthai (1989) collected a large amount of structural data from the central Argolis area indicating emplacement from the northeast, a result confirmed by our own data.

The polyphase deformational history of the ophiolite has made the singling out of emplacement-related structures difficult. Paleogene rethrusting from southeast to northwest and Neotectonic normal faulting have each overprinted the earlier structures. In an attempt to restrict structural measurements to Jurassic structures alone all structures with a Neotectonic or Paleogene (E-W) strike were discounted. The folding of ribbon cherts both within the ophiolite sedimentary cover and at the top of the Pantokrator Unit, is considered to be obduction related, due to the present brittle nature of these rocks and the resultant improbability that they could have been deformed into small-scale isoclinal folds following diagenesis. Since deposition of radiolarian cherts on the Pelagonian platform is curtailed by obduction of the ophiolite, it may be assumed that these sediments would still have been soft at this time and liable to folding. Importantly, where observed, folds in radiolarian cherts show only one ductile deformational episode, which is inconsistent with known post-Jurassic structural trends.

Tab. 1. X-ray fluorescence analyses of lavas from the Migdhalitsa Ophiolite.

|                                | Moderate Nb      |                  |                  |                  |                  |                  |                  |                  |                  |                  |              |              |              | Evolved Moderate Nb |                  |                  |                  |
|--------------------------------|------------------|------------------|------------------|------------------|------------------|------------------|------------------|------------------|------------------|------------------|--------------|--------------|--------------|---------------------|------------------|------------------|------------------|
|                                | AR-84<br>-188, 1 | AR-84<br>-188, 2 | AR-84<br>-191, 1 | AR-84<br>-191, 2 | AR-84<br>-191, 5 | AR-84<br>-195, 3 | AR-84<br>-206, 1 | AR-84<br>-206, 2 | AR-84<br>-206, 3 | AR-84<br>-206, 4 | AR-89<br>-59 | AR-89<br>-60 | AR-89<br>-69 | AR-84<br>-188, 3    | AR-84<br>-188, 4 | AR-84<br>-191, 3 | AR-84<br>-191, 4 |
| SiO <sub>2</sub>               | 37,93            | 38,64            | 49,95            | 43,66            | 49,11            | 44,78            | 49,17            | 46,74            | 50,43            | 49,45            | 46,48        | 42,28        | 43,63        | 49,87               | 52,29            | 44,65            | 44,24            |
| Al <sub>2</sub> O <sub>3</sub> | 11,19            | 10,78            | 15,06            | 13,24            | 14,93            | 14,97            | 13,99            | 13,38            | 13,23            | 13,84            | 14,68        | 14,75        | 12,16        | 12,2                | 12,62            | 14,78            | 16,27            |
| Fe <sub>2</sub> O <sub>3</sub> | 4,93             | 4,98             | 10,14            | 7,47             | 8,95             | 8,66             | 8,89             | 9,15             | 9,13             | 8,84             | 8,27         | 8,33         | 8,31         | 8,38                | 8,97             | 12,55            | 10,8             |
| MgO                            | 5,07             | 5,05             | 5,83             | 6,18             | 6,91             | 8,7              | 6,51             | 6,74             | 6,99             | 6,69             | 7,36         | 6,87         | 5,55         | 4,32                | 4,5              | 2,55             | 4,22             |
| CaO                            | 21,87            | 22,22            | 10,36            | 14,03            | 9,96             | 8,87             | 10,83            | 13,1             | 11,34            | 11,22            | 10,83        | 13,18        | 15,55        | 11,36               | 9,29             | 9,86             | 7,66             |
| Na <sub>2</sub> O              | 2,48             | 3,57             | 3,6              | 3,34             | 3,1              | 4,12             | 4,66             | 4,01             | 4                | 4,47             | 3,97         | 3,67         | 3,47         | 6,1                 | 6,36             | 3,58             | 5,5              |
| K <sub>2</sub> O               | 1,41             | 0,08             | 1,17             | 1,4              | 2,02             | 0,91             | 0,04             | 0,03             | 0,02             | 0,03             | 0,853        | 0,424        | 1,294        | 0,17                | 0,16             | 2,3              | 1,22             |
| TiO <sub>2</sub>               | 0,66             | 0,62             | 1,28             | 0,97             | 1,28             | 0,86             | 1,31             | 1,32             | 1,33             | 1,33             | 1,19         | 1,236        | 1,019        | 1,15                | 1,26             | 2,14             | 1,31             |
| MnO <sub>2</sub>               | 0,21             | 0,18             | 0,14             | 0,15             | 0,17             | 0,25             | 0,17             | 0,18             | 0,15             | 1,15             | 0,155        | 0,154        | 0,092        | 0,12                | 0,13             | 0,21             | 0,17             |
| P <sub>2</sub> O <sub>5</sub>  | 0,12             | 0,12             | 0,21             | 0,12             | 0,2              | 0,1              | 0,19             | 0,18             | 0,2              | 0,18             | 0,24         | 0,251        | 0,234        | 0,16                | 0,16             | 0,46             | 0,16             |
| LOI                            | 14               | 13,6             | 2                | 9,5              | 3,5              | 6,8              | 3,8              | 4,7              | 2,6              | 3,5              | 5,81         | 8,11         | 8,74         | 5,8                 | 4,2              | 6,5              | 8,6              |
| Total                          | 99,87            | 99,84            | 99,74            | 100,06           | 100,13           | 99,02            | 99,56            | 99,53            | 99,42            | 100,70           | 99,84        | 99,26        | 100,05       | 99,63               | 99,94            | 99,58            | 100,15           |
| Ni                             | 117              | 1,09             | 82               | 73               | 97               | 119              | 83               | 84               | 86               | 85               | 93,7         | 89,9         | 201          | 63                  | 74               | 30               | 158              |
| Cr                             | 279              | 254              | 274              | 227              | 215              | 313              | 271              | 270              | 259              | 279              | 199,8        | 176,7        | 596,4        | 215                 | 251              | 6                | 371              |
| V                              | 191              | 185              | 294              | 208              | 274              | 214              | 289              | 297              | 288              | 299              | 300,9        | 311,2        | 223          | 250                 | 272              | 406              | 221              |
| Sc                             | 17               | 12               | 41               | 28               | 37               | 35               | 38               | 42               | 38               | 37               | 39,6         | 38,1         | 30,6         | 22                  | 33               | 34               | 35               |
| Cu                             | 81               | 74               | 76               | 38               | 29               | 90               | 70               | 78               | 74               | 72               | 72,3         | 45,6         | 31,3         | 27                  | 31               | 38               | 73               |
| Zn                             | 52               | 57               | 78               | 55               | 73               | 57               | 73               | 79               | 84               | 76               | 64,2         | 65,9         | 63,9         | 64                  | 74               | 107              | 112              |
| Sr                             | 80               | 79               | 220              | 79               | 295              | 103              | 108              | 87               | 103              | 103              | 463          | 338          | 182          | 55                  | 50               | 224              | 112              |
| Rb                             | 6                | 1                | 15               | 21               | 21               | 11               | 0                | 0                | 0                | 0                | 16,8         | 8,5          | 19           | 3                   | 2                | 34               | 24               |
| Zr                             | 41               | 40               | 79               | 52               | 82               | 48               | 85               | 85               | 86               | 85               | 75,2         | 78           | 73,3         | 77                  | 84               | 151              | 97               |
| Nb                             | 7                | 7                | 21               | 7                | 22               | 7                | 14               | 14               | 15               | 14               | 19           | 20,1         | 15,8         | 8                   | 9                | 37               | 6                |
| Ba                             | 113              | 21               | 143              | 58               | 244              | 165              | 57               | 26               | 49               | 42               | 81,4         | 60,4         | 94,4         | 26                  | 26               | 184              | 74               |
| Pb                             | 14               | 8                | 1                | 1                | 2                | 2                | 1                | 3                | 2                | 1                |              |              |              | 1                   | 1                | 2                | 1                |
| Th                             | 1                | 1                | 1                | 1                | 2                | 0                | 1                | 1                | 1                | 2                |              |              |              | 1                   | 0                | 2                | 0                |
| La                             | 10               | 8                | 15               | 0                | 13               | 5                | 11               | 9                | 13               | 11               | 18,4         | 18,4         | 16           | 9                   | 12               | 26               | 10               |
| Ce                             | 17               | 19               | 19               | 12               | 31               | 15               | 27               | 20               | 32               | 32               | 35,5         | 29,5         | 25,6         | 20                  | 17               | 54               | 14               |
| Nd                             | 14               | 13               | 19               | 7                | 13               | 6                | 15               | 14               | 19               | 13               | 16           | 15,3         | 14,2         | 10                  | 10               | 21               | 9                |
| Y                              | 15               | 16               | 22               | 20               | 21               | 19               | 27               | 27               | 28               | 28               | 18,3         | 18,2         | 16,1         | 23                  | 27               | 37               | 27               |

Figure 12a shows poles to brittle shear fabrics within massive and pillowed basalts in the Migdhalitsa type area. Assuming that these were formed as small imbricate thrusts this implies that the sense of shear within the nappe as a whole would be consistent with overthrusting in the opposite direction to the dip direction of the shear zone, i.e. the same direction as the azimuth of the poles to the shear fabric. While back rotation due to Neotectonic faulting and reverse dipping duplexes will disrupt this simple pattern these points should still plot on a great circle, whose bisector around the stereographic equator should still lie along the line of emplacement. In the case of the Migdhalitsa area the shear fabrics demonstrate a sense of shearing consistent with an overthrusting towards the SW. Figure 12b reinforces this result by showing fold hinge axes for deformed ribbon radiolarites, both from the sedimentary cover of the ophiolite and the underlying Pantokrator Unit. It shows that the sense of asymmetry, coupled with the younging direction, when known, is again consistent with overthrusting to-

wards the SSW. As a third line of evidence, Figure 12c displays dip and azimuth of slickensides on selected fault planes associated to the brittle shear zones mentioned above within the Migdhalitsa type area. Stepping of the fault planes, as well as the accumulation of fault breccia on the lee side of positive features on the fault plane act as criteria to determine the sense of motion (see Petit 1987), which indicate an overthrusting towards the SSW for the Migdhalitsa Ophiolite.

In conclusion we infer that the present structural evidence indicates that the Migdhalitsa Ophiolite of the central Argolis area was emplaced from the present NE-NNE towards the SW-SSW. In contrast to this data Photiades (1986) presented structural information from southern Argolis (Kouverta; Fig. 1) indicating that serpentinites and radiolarian cherts in that area were folded in Upper Jurassic times along an E-W axis (80-90°). While this implies an apparently anomalous N-S emplacement direction paleomagnetic data discussed below shows that this area is in accord with the central type region.

Tab. 2. ICP-MS analyses of the rare earth elements of selected Migdhalitsa Ophiolite lavas.

| Elements | AR-88<br>-159 | AR-88<br>-161 | AR-88<br>-163 | AR-84<br>-195-1 | AR-84<br>-195-2 | AR-84<br>-195-3 | AR-84<br>-195-4 | AR-84<br>-195-5 | AR-206<br>-4 |
|----------|---------------|---------------|---------------|-----------------|-----------------|-----------------|-----------------|-----------------|--------------|
| La       | 3,69          | 4,68          | 4,01          | 5,99            | 5,22            | 5,84            | 5,74            | 16,94           | 13,04        |
| Ce       | 10,92         | 13,77         | 13,44         | 14,08           | 12,75           | 13,72           | 13,45           | 31,31           | 28,16        |
| Pr       | 1,63          | 2,18          | 1,85          | 1,76            | 1,74            | 1,77            | 1,70            | 3,91            | 3,47         |
| Nd       | 9,33          | 11,63         | 9,42          | 7,89            | 7,42            | 7,74            | 7,84            | 15,04           | 14,34        |
| Sm       | 3,32          | 4,15          | 3,18          | 2,32            | 2,30            | 2,22            | 2,29            | 3,70            | 3,80         |
| Eu       | 1,28          | 1,49          | 1,19          | 0,85            | 0,80            | 0,76            | 0,84            | 1,21            | 1,28         |
| Gd       | 4,59          | 5,69          | 4,18          | 2,92            | 2,92            | 2,84            | 2,86            | 3,87            | 4,54         |
| Dy       | 5,82          | 7,23          | 4,96          | 3,44            | 3,45            | 3,34            | 3,48            | 4,27            | 5,36         |
| Ho       | 1,08          | 1,34          | 0,91          | 0,63            | 0,63            | 0,63            | 0,64            | 0,76            | 0,97         |
| Er       | 3,30          | 4,21          | 2,77          | 1,94            | 1,96            | 1,93            | 1,97            | 2,24            | 3,02         |
| Yb       | 3,03          | 3,87          | 2,55          | 1,79            | 1,81            | 1,80            | 1,80            | 2,10            | 2,80         |
| Lu       | 0,43          | 0,56          | 0,36          | 0,24            | 0,26            | 0,26            | 0,26            | 0,30            | 0,40         |

## Discussion

With regard to the large scale tectonic implications of the Migdhalitsa Ophiolite for the Hellenides, any interpretation made using the structural data presented above can only be made after consideration of the paleomagnetically determined rotation of the peninsula since emplacement. Turnell (1988) demonstrated that the Argolis Peninsula has undergone approximately 70° of clockwise rotation since the mid Jurassic. This, and a multitude of new measurements, indicate  $\leq 107^\circ$  rotation of central Argolis, averaging approximately 90° since this time (Morris 1990). This implies that the restored direction of emplacement would have been from the NW–WNW in Kimmeridgian times for the central area. Lesser degrees of rotation (45° clockwise; Morris 1990) in the southern Argolis area furthermore restore the N-S emplacement direction of Photiades (1986) to be NW-SE for the Kimmeridgian, in agreement with the central region. However, clockwise rotation of other Greek isopic zones by approximately 50° since this time (pers. comm., A. Morris 1996) means that the direction of emplacement of the ophiolite seems to have been obliquely from the Pindos Zone.

In the case of several other Greek ophiolites the direction of emplacement is also unclear, although the age of emplacement would also seem to be the same for all known cases; e.g. Kimmeridgian for the ophiolite units on Euboea (De Wever 1982). Thus while the age data allow for the possibility of two separate ophiolite thrust sheets being emplaced on to the Pelagonian microcontinent from different directions, effectively synchronously, a Pindos Zone source for all the Subpelagonian ophiolites of southern and central Greece is possible and more probable, given available structural information from Euboea (Robertson 1990), Pindos (Jones et al. 1991) and from the Othris Mountains (Smith et al. 1979). The lithological, tectonic and geochemical similarities of the Migdhalitsa Ophiolite with a number of these other ophiolites, especially the As-

propotamos Complex of the Pindos Mountain thrust stack, suggests a common origin in a western Tethyan basin.

As far as ophiolite obduction in general is concerned, the data from the Argolis Peninsula provide a number of constraints to the settings in which these features may form:-

- (1) Ophiolite genesis began with the creation of the Migdhalitsa Ophiolite at a slow spreading ocean ridge within the relatively narrow Pindos strand of the Mesozoic Tethys.
- (2) Slowing and cessation of spreading was followed by collapse and overthrusting close to or at the ridge. There is no strong suggestion of subduction initiation related to a pre-existing fracture zone. This process left the Migdhalitsa Ophiolite in a forearc position, where it was intruded by boninitic magmas. The major, subduction-influenced, Hellenic ophiolites (e.g. Pindos and Vourinos) were then generated immediately after subduction initiation in a supra-subduction zone setting.
- (3) Collision of the passive margin to the Pelagonian continent with the trench caused flexural collapse and obduction of the ophiolite. Obduction was not linked to continent/continent or arc/continent collision. In many obduction events overthrusting results in the tectonic excision and loss of the forearc slice, e.g. Semail Ophiolite, Oman, although in Argolis this has not occurred. Deformation related to ophiolite obduction was principally thin skinned in character.

## Acknowledgments

This work was carried out through the help of S. P. Varnavas, Patras University. PC's work was supported by the Natural Environment Research Council and by Woods Hole Oceanographic Institution. A.H.F. Robertson, G. Jones, T. Ustaomer and A. Morris are thanked for their discussions on the tectonics of the Aegean region. J. G. Fitton and D. James provided excellent facilities and advice on XRF analyses, while N. Walsh at Royal Holloway and Bedford New College is thanked for his help with ICP analyses. I. Pecher is thanked for his help in translating the abstract into German. This is WHOI contribution number 9618.

## REFERENCES

- AUBOUIN, J., BONNEAU, M., CELET, P., CHARVET, J., CLÉMENT, B., DEGARDIN, J. M., DERCOURT, J., FERRIÈRE, J., FLEURY, J. J., GUERNET, C., MAILLOT, H., MANIA, J., MANSY, J. L., TERRY, J., THIEBAULT, P., TSOFLIAS, P. & VERRIEUX, J. J. 1970: Contribution à la géologie des Hellenides: Le Gavrovo, le Pinde et la Zone Ophiolitique Subpélagonienne. *Ann. Soc. Géol. Nord* 90, 277–306.
- BASALTIC VOLCANISM STUDY PROJECT, 1981: Basaltic volcanism on the terrestrial planets. New York: Pergamon Press, p.1286.
- BAUMGARTNER, P. O. 1985: Jurassic sedimentary evolution and nappe emplacement in the Argolis Peninsula (Peloponnesus, Greece). *Mem. Soc. Helv. Sci. Nat.*, 111 pp.
- Beccaluva, L., Ohnenstetter, D., Ohnenstetter, M. & Paupy, A. 1984: Two magmatic series with island arc affinities within the Vourinos Ophiolite. *Contrib. Mineral. Petrol.* 85, 253–271.
- BERNOULLI, D. & LAUBSCHER, H. 1972: The palinspastic problem of the Hellenides. *Ecolae geol. Helv.* 67, 107–118.
- BLOOMER, S. H., TAYLOR, B., MACLEOD, C. J., STERN, R. J., FRYER, P., HAWKINS, J. W., & JOHNSON, L. 1995: Early arc volcanism and the ophiolite problem: perspective from drilling in the western Pacific. In: Active margin and marginal basins of the western Pacific (Ed. by TAYLOR, B., & NATLAND, J.). *Monogr. Amer. Geophys. Union* 88, 1–30.
- CAMERON, W. E., NISBET, E. G. & DIETRICH, V. J. 1979: Boninites, Komatiites and Ophiolite Basalts. *Nature* 280, 550–553.
- CASEY, J. F., & DEWEY, J. F. 1984: Initiation of subduction zones along transform and accreting plate boundaries, triple junction evolution, and forearc spreading centres-implications for ophiolite geology and obduction. In: Ophiolites and oceanic lithosphere (Ed. by GASS, I. G., LIPPARD, S. J., & SHELTON, A. W.). *Geol. Soc. (London) spec. publ.* 13, 269–290.
- CELET, P. & FERRIÈRE, J. 1978: Les Hellenides internes: Le Pélagonien. *Ecolae geol. Helv.* 73, 467–495.
- CLIFT, P. D. & ROBERTSON, A. H. F. 1989: Evidence of a late Mesozoic ocean basin and subduction/accretion in the southern Greek Neotethys. *Geology* 17, 559–563.
- 1992: Collision tectonics of the Greek Neotethys. *Geol. Rdsch.* 81 (3), 669–679.
- COLEMAN, R. G. 1977: Ophiolites: Ancient oceanic lithosphere? Springer, New York.
- COX, K. G., BELL, J. D. & PANKHURST, R. J. 1979: The Interpretation of Igneous Rocks. George Allen and Unwin, London.
- CRAWFORD, A. J. 1989: Boninites. Unwin Hyman.
- DAL PIAZ, G. V., MARTIN, S., VILLA, I. M., GOSSO, G., & MARSHALCO, R. 1995: Late Jurassic blueschist facies pebbles from the western Carpathian orogenic wedge and paleostructural implications for western Tethys evolution. *Tectonics* 14 (4), 874–885.
- DEGNAN, P. J. & ROBERTSON, A. H. F. 1991: Tectonic and sedimentary evolution of the western Pindos Ocean: N.W. Peloponnese, Greece. *Bull. Geol. Soc. Greece* 25, (1), 263–273.
- DERCOURT, J., RICOU, L. E., ADAMIA, SH. A., CSASZAR, G., FUNK, H., LEFELD, J., RAKUS, M., SANDULESCU, M., TOLLMAN, A. & TCHOUMATCHENCKO, P. 1990: Northern margin of Tethys: Paleogeographic maps. *Geol. Ustav Dionyza Stura, Bratislava, Czechoslovakia (IGCP Project 198)*, 11 sheets.
- DEWEY, J. F. & BIRD, J. M. 1971: Origin and emplacement of the ophiolite suite: Appalachian ophiolites in Newfoundland. *J. geophys. Res.* 76, 3179–3206.
- DE WEVER, P. 1982: Geological Map of Greece, 1/50,000. Kandhila Sheet. *Inst. Geol. Min. Expl.*, Athens.
- DICK, H. J. B. 1989: Abyssal peridotites, very slow spreading ridges and ridge magmatism. In: Magmatism in the Ocean Basins (Ed. by SAUNDERS, A. D. & NORRY, M. J.), *Geol. Soc. (London) spec. publ.* 42, 71–106.
- DIETRICH, V. J., OBERHAENSLI, R. & MERCOLLI, I. 1987: A new occurrence of boninite from the ophiolitic mélange in the Pindus-Sub-Pelagonian Zone S.L.: Aegina island, Saronic Gulf, Greece. *Ophioliti* 12 (1), 83–90.
- DOSTAL, J., TOSCANI, L., PHOTIADES, A. & CAPEDEI, S. 1991: Geochemistry and petrogenesis of Tethyan ophiolites from northern Argolis (Peloponnesus, Greece). *Europ. J. Min.* 3, 105–121.
- DOUTSOS, T., PE-PIPER, G., BORONKAY, K., & KOUKOUVELAS, I. 1993: Kinematics of the central Hellenides. *Tectonics* 12, 936–953.
- FITTON, J. G., SAUNDERS, A. D., NORRY, M. J., & HARDARSON, B. S., 1997: Thermal and chemical structure of the Iceland Plume. *Earth and planet. Sci. Lett.*, in press.
- FLEURY, J. J. 1980: Les zones de Gavrovo-Tripolitza et du Pinde-Olonos (Grèce continentale) et Peloponèse du Nord. Evolution d'une plate-forme et d'un bassin dans leurs cadre alpin. *Soc. Geol. Nord, Lille* 4, 1–651.
- GASS, I. G. & MASSON-SMITH, D. 1963: The geology and gravity anomalies of the Troodos massif, Cyprus. *Phil. Trans. r. Soc. London* A255, 417–467.
- GREEN, T. J. 1983: The sedimentology and structure of the Pindos Zone in southern mainland Greece. Ph.D. thesis, University of Cambridge, UK.
- HEKINIAN, R., FEVRIER, M., AVEDIK, F., CAMBON, P., CHARLOU, J. L., NEEDHAM, H. D., RAILLARD, J., BOULEGUE, J., MERLIVAT, L., MOINET, A., MANGANINI, S. & LANGE, L. 1983: East Pacific Rise near 13°N: Geology of new hydrothermal fields. *Science* 219, 1321–1324.
- HUSSONG, D. M. & UYEDA, S. 1981: Tectonic Processes and the history of the Mariana Arc: A synthesis of the results of the Deep Sea Drilling Project Leg 60. *Init. Rep. Deep Sea Drill. Proj.* 60, 909–929.
- HYNES, A. 1974: Igneous activity at the birth of an oceanic basin in Eastern Greece. *Can. J. Earth Sci.* 11, 842–853.
- JONES, G. & ROBERTSON, A. H. F. 1991: Tectono-stratigraphy and evolution of the Mesozoic Pindos ophiolite and related units, northwestern Greece. *J. geol. Soc., (London)* 148 (2), 267–288.
- JONES, G., ROBERTSON, A. H. F. & CANN, J. R. 1991: Supra-subduction zone origin of the Pindos Ophiolite, northwestern Greece. In: Ophiolite Genesis and Evolution of the Oceanic Lithosphere (Ed. by PETERS, T., NICOLAS, A. & COLEMAN, R. G.), Kluwer Press, 779–807.
- KARSON, J. & DEWEY, J. F. 1978: Coastal complex, western Newfoundland; an early Ordovician oceanic fracture zone. *Bull. Geol. Soc. Amer.* 89, 1037–1049.
- KLEIN, E. M. & LANGMUIR, C. H. 1987: Global correlation of ocean ridge basalt chemistry with axial depth and crustal thickness. *J. geophys. Res.* 92, 8089–8115.
- KOSTOPOULOS, D. 1989: Geochemistry and Tectonic Setting of the Pindos Ophiolite, northwest Greece. Unpublished Ph.D. thesis, University of Newcastle-upon-Tyne.
- LATIN, D. M., DIXON, J. E. & FITTON, J. G. 1990: Rift-Related Magmatism in the North Sea Basin. In: Tectonic Evolution of the North Sea Rifts (Ed. by BLUNDELL, D. J. & GIBBS, A.), Oxford Univ. Press.
- LIPPARD, S. J., SHELTON, A. W. & GASS, I. G. 1986: The Ophiolite of Northern Oman. *Geol. Soc., (London) Mem.* 11, p.178.
- MALPAS, J. 1979: The dynamothermal aureole of the Bay of Islands ophiolite suite. *Can. J. Earth Sci.* 16, 2086–2101.
- MATTHAI, S. K. 1989: Kartierung und strukturgeologische Untersuchungen im Gebiet Vothiki-Stavropodi, Argolis Halbinsel (Griechenland). Unpublished M.Sc. thesis, University of Tübingen, Germany.
- MCKENZIE, D. P. & BICKLE, M. 1988: The volume and composition of melt generated by extension of the lithosphere. *J. Petrol.* 29, 625–679.
- MORRIS, A. 1990: Palaeomagnetic studies of the Mesozoic-Tertiary tectonic evolution of Cyprus, Turkey and Greece. Unpublished Ph.D. thesis, University of Edinburgh. p. 335.
- NATLAND, J. H. & TARNEY, J. 1979: Petrological evolution of the Mariana arc and backarc basin system- a synthesis of drilling in the south Philippine sea. *Init. Rep. Deep Sea Drill. Proj.*, 60, 877–909.
- NISBET, E. G. & FOWLER, C. M. R. 1978: The Mid Atlantic Ridge at 37 and 45 degrees north: some geophysical and petrological constraints. *Geophys. J. R. Astro. Soc.* 54, 631–60.
- NOIRET, G., MONTIGNY, R. & ALLÈGRE, C. J. 1981: Is the Vourinos Complex an island arc ophiolite? *Earth and planet. Sci. Lett.* 56, 375–386.
- PEARCE, J. A. 1982: Trace element characteristics of lavas from destructive plate boundaries. In: Andesites (Ed. by THORPE, R. S.), 57–75, John Wiley and Sons.
- PETIT, J. P. 1987: Criteria for the sense of movement on fault surfaces in brittle rocks. *J. Struct. Geol.*, 9 (5/6), 597–608.
- PE-PIPER, G. & PIPER, D. J. W. 1984. Tectonic setting of the Mesozoic Pindos Basin of the Peloponnese, Greece. In: Geological Evolution of the East-

- ern Mediterranean (Ed. by DIXON, J. E. & ROBERTSON, A. H. F.). Geol. Soc. (London) spec. publ. 17, 563–568.
- PHOTIADES, A. 1986: Contribution à l'étude géologique et métallogénique des unités ophiolitiques de l'Argolide septentrionale (Grèce). Unpublished Ph.D. thesis, University of Besançon, p. 261.
- 1989: The diversity of the Jurassic volcanism in the inner parts of the Hellenides. Bull. Geol. Soc. Greece 23 (2), 515–530.
  - ECONOMOU, G. & KATSIKIS, J. 1989: Etude minéralogique des clinopyroxènes associés aux roches volcaniques des unités ophiolitiques de l'Argolide Septentrionale (Peloponnèse, Grèce). Bull. Geol. Soc. Greece 23 (2), 499–514.
- ROBERTSON, A. H. F. & DIXON, J. E. 1984: Introduction: aspects of the geological evolution of the Eastern Mediterranean. In: The Geological Evolution of the Eastern Mediterranean (Ed. by DIXON, J. E. & ROBERTSON, A. H. F.), Geol. Soc., (London) spec. publ. 17, 1–74.
- VARNAVAS, S. P. & PANAGOS, A. G. 1987: Ocean ridge origin and tectonic setting of Mesozoic sulphide and oxide deposits of the Argolis Peninsula of the Peloponnesus, Greece. Sediment. Geol. 53, 1–32.
  - 1990: New evidence of Late Cretaceous oceanic crust emplaced over an Early Tertiary foreland basin: Euboea, Eastern Greece. Terra Nova 2, 333–339.
  - CLIFT, P. D., JONES, G. & DEGNAN, P. J. 1991: The palaeoceanography of the Eastern Mediterranean Neotethys. Palaeocean. Palaeoclim., Palaeoecol. 87, 289–344.
- ROMERMANN, H. 1968: Geologie von Hydra. Geol. Palaeont. 2, 163–171.
- SCOTT, M. R., SCOTT, R. B., RONA, P. A., BUTLER, L. W. & NALWALK, A. J. 1974: Rapidly accumulating manganese deposit from the median valley of the Mid-Atlantic Ridge. Geophys. Res. Lett. 1, 355–358.
- SEARLE, M. P. & MALPAS, J. 1982: Petrochemistry and origin of sub-ophiolitic metamorphic and related rocks in the Oman Mountains. J. Geol. Soc. (London) 139, 235–248.
- SMITH, A. G., WOODCOCK, N. H., & NAYLOR, M.A. 1979: The structural evolution of a Mesozoic continental margin. J. Geol. Soc. (London) 136, 589–603.
- SPRAY, J. G., 1983: Lithosphere-asthenosphere decoupling at spreading centres and initiation of obduction. Nature 304, 253–255.
- SUN, S.-S. & McDONOUGH, W. 1989: Chemical and isotopic systematics of oceanic basalts; implications for mantle composition and processes. In: Magmatism in the Ocean Basins (Ed. by SAUNDERS, A. D. & NORRY, M. J.), Geol. Soc., (London) spec. publ. 42, 324–356.
- SUN, S.-S., NESBITT, R. W. & SHARASKIN, Y. A. 1979: Geochemical characteristics of mid-ocean ridge basalts. Earth and planet. Sci. Lett. 44, 119–38.
- TURNELL, H. B. 1988: Mesozoic evolution of Greek microplates from paleomagnetic measurements. Tectonophysics 155, 307–316.
- VACHARD, D., CLIFT, P. D., & DECROUEZ, D. 1993: Une association à *Pseudodunbarula* (fusulinoïde) du Permien supérieur (Djoulfien) remaniée dans le Jurassique d'Argolide (Peloponnèse, Grèce). Rev. Paleobiol. 12, 217–242.
- VRIELYNCK, B. 1982: Evolution paléogéographique et structurale de la presqu'île d'Argolide (Grèce). Rév. Géol. Dyn. Géograph. Phys. 23, 277–288.
- WILLIAMS, H. 1975: Structural succession, nomenclature and interpretation of transported rocks in Western Newfoundland. Can. J. Earth Sci. 12, 1874–1894.
- WOODCOCK, N. H. & ROBERTSON, A. H. F. 1977: Origins of some ophiolite-related metamorphic rocks of the "Tethyan" belt. Geology 5, 373–376.
- ZIEGLER, P. A. 1988. Post-Hercynian plate reorganization in the Tethys and Arctic-North Atlantic domain. In: Triassic-Jurassic rifting; continental breakup and the origin of the Atlantic Ocean and passive margins (Ed. by MANSPEIZER, W.), Elsevier, Amsterdam, 711–755.

Manuscript received June 17, 1997  
Revision accepted December 22, 1997